Journal of Environmental Sciences Vol.17, No.1, pp.76—80, 2005

ISSN 1001—0742
CN11—2629/X

Article ID: 1001-0742(2005)01-0076-05 **CLC number**: X13; O643.3 **Document code**: A

Visible light induced photodegradation of organic pollutants on nitrogen and fluorine co-doped TiO_2 photocatalyst

WANG Zheng-peng, XU Jun, CAI Wei-min*, ZHOU Bao-xue, HE Zheng-guang, CAI Chun-guang, HONG Xiao-ting

(School of Environmental Science and Engineering, Shanghai Jiaotong University, Shanghai 200240, China. E-mail: wizip@sjtu.edu.cn)

Abstract: The nitrogen and fluorine co-doped TiO_2 polycrystalline powder was synthesized by calcinations of the hydrolysis product of tetra-butyl titanate with ammonium fluoride. Nitrogen and fluorine co-doping causes the absorption edge of TiO_2 to shift to a lower energy region. The photocatalytic activity of co-doped TiO_2 with anatase phases was found to be 2.4 times higher than that of the commercial TiO_2 photocatalyst Degussa P25 for phenol decomposition under visible light irradiation. The co-doped TiO_2 powders only contain anatase phases even at 1000℃. Apparently, ammonium fluoride added retarded phase transformation of the TiO_2 powders from anatase to rutile. The substitutional fluorine and interstitial nitrogen atoms in co-doped TiO_2 polycrystalline powder were responsible for the vis light response and caused the absorption edge of TiO_2 to shift to a lower energy region.

Keywords: photocatalyst; visible light; nitrogen and fluorine co-doped; phenol; band gap

Introduction

Titanium dioxide (TiO_2) has been extensively investigated for its catalytic properties based on its wide applications as environmentally harmonious photocatalysts (Fujishima, 1972; Asahi, 2001). Nevertheless, TiO_2 becomes active only by irradiating with ultraviolet(UV) light. The modification of TiO_2 sensitive to visible light is one of the current topic in photocatalyst field. In previous studies, the doping with various transition metals has been intensively employed to extend the light absorption to the visible region. Iwasaki *et al*. (Iwasaki, 2000) substituted Co^{2+} at lattice positions of Ti^{4+} in TiO_2 by sol-gel method. They observed that TiO_2 doped with Co^{2+} ions has highly photocatalytic activities under vis light irradiation, and considered that the photocatalytic activity under vis light irradiation strongly depends on the valence state of Co ions in the dopant and its concentration rather than the specific surface area and the crystallinity of anatase. Except for a few cases (Yamashita, 1999; 2001), however, the photocatalytic activities of the cation-doped TiO_2 decreased even in the UV region. This is because the doped oxides suffer from a thermal instability or an increase in the carrier-recombination centers (Choi, 1994; Herrmann, 1984).

Recently, there are some reports that films and powders of anion doped TiO_2 have photoactivity under visible light. Asahi *et al*. (Asahi, 2001) insisted that the oxygen sites were substituted by nitrogen atoms and that these nitrogens were responsible for the vis light sensitivity by theoretically calculating the band structure of the nitrogen-doped TiO_2 powders and thin films. In addition, Asahi concluded that the vis light sensitivity of the nitrogen-doped TiO_2 was due to the narrowing of the band gap by mixing the N 2p and O 2p states. Umebayashi *et al*. (Umebayashi, 2002) reported that the S-doped TiO_2 was synthesized by oxidation annealing of titanium disulfide (TiS_2). They concluded the S doping caused the absorption edge of TiO_2 to be shifted into the lower-energy region by mixing of the S 3p states with the valence band according to the theoretical analyses using *ab initio* band calculations. Carbon doped TiO_2 was reported as a water oxidation material under vis light irradiation. Khan *et al*. (Khan, 2002) asserted that carbon atoms substituted for some of the lattice oxygen atoms. Yamaki *et al*. (Yamaki, 2002; 2003) reported that the $TiO_{2-x}F_x$ was synthesized by ion implantation technique, and they concluded that the F doping gave rise to modification of the electronic structure around the conduct band edge of TiO_2 by using the FLAPW method calculations.

It is clear that N, C, S, and F-doping for oxygen in TiO_2 could narrow the band gap, possibly leading to new visible light-driven photocatalysts. However, to our knowledge, the effects of nitrogen and fluorine elements co-doping and heat treatment on photocatalytic activity and microstructures of nanocrystalline TiO_2 powders have not been reported. In this study, we incorporated nitrogen and fluorine into TiO_2 by hydrothermal synthesis using tetra-butyl titanate ($Ti(OBu)_4$) as the titanium source in the ammonium fluoride (96%) solution. With the calcination temperature rising from 250℃ to 1000℃, only pure anatase phases were obtained. The photocatalyst was found to be very active for phenol decomposition under visible light irradiation compared to commercial TiO_2 photocatalyst Degussa P-25 (P25). We concluded that the nitrogen and fluorine atoms in TiO_2 were shown to contribute to the band gap narrowing and enhance the photocatalytic activity for phenol decomposition under visible light (wavelength < 700 nm). In comparison with conventional synthesis reaction, the present synthesis method is mild, convenient and easy to handle. This work may provide new insights and understanding on the mechanisms of

photoactivity enhancement by nitrogen and fluorine co-doping into the lattice of TiO_2.

1 Experimental

1.1 Photocatalyst synthesis

Eight ml ammonium fluoride(96%) solution was added dropwise into 20 ml tetra-butyl titanate($Ti(OBu)_4$) solution (99%) at room temperature under roughly stirring by a stirrer to carry out hydrolysis. After continuously stirring for 10 min, the precursor was naturally dried in an oven at 100℃ for 0.5 h in air. Finally, the TiO_2 precursor was calcined at different temperature for 2 h to obtain different TiO_2 nanoparticles. The color of the sample powder was changed from white to brown at different temperature. The color of this photocatalyst in 375℃ was brown and absorbed visible light intensively. The tetra-butyl titanate and the ammonium fluoride were obtained from Shanghai Reagent Corporation, in China. The commercial TiO_2 photocatalyst Degussa P-25 was supplied by Germany Degussa Co. Ltd.

1.2 Characterization

XRD patterns obtained on a Bruker AXS D8 Discover with GADDS X-ray diffractometer using Cu K_α radiation as X-ray source were used to determine the crystallite size and identity. The accelerating voltage and the applied current were 35 kV and 20 mA, respectively. The average crystallite sizes of anatase were determined according to the Scherrer equation using the full width at half maxima(FWHM) data of each phase after correcting the instrumental broadening. Sizes and shapes were observed using transmission electron microscopy (TEM) (JEOL JEM-100CX, Japan). The Brunauer-Emmett-Teller(BET) surface area(SBET) and pore size distribution were determined using a Micromeritics ASAP 2010 nitrogen adsorption apparatus. All the samples were degassed at 180℃ prior to BET measurements. UV-Vis absorption spectra of TiO_2 powders were obtained for the dry pressed disk samples using a UV-Vis spectrophotometer(Cary 500 Scan Spectrophotometers, Varian, U. S. A.). XPS measurement was carried out on a VG Scientific Microlab 310F system using Mg K_α (1253.6 eV) radiation as X-ray source. All the binding energies were referenced to the C 1s peak at 285 eV of the surface adventitious carbon.

1.3 Photoactivity measurement.

The photocatalytic activity of the N-doped TiO_2 powders was evaluated according to the photodegradation of phenol aqueous solutions. Phenol is a common chemical used extensively in a variety of industrial and agricultural applications, and was, therefore, chosen as a model contaminant. 1000 ml 20 ppm phenol aqueous solution with 0.50 g sample powders was loaded in a glass container and stirred with a magnetic stirrer under the irradiation of 1000 W xenon lamp. A 400 nm glass filter was used to assure cutoff of the UV light. The temperature of the photoreactor was maintained at 20℃. It was found that the phenol concentration had not changed significantly after 30 min. We then began irradiation. The phenol concentration as a function of time was measured using the colorimetric method of 4-aminoantipyrine with UNICO UV-2102PCS spectrophotometer after filtration under reduced pressure. The photocatalytic behavior of Degussa P-25 (P25) was also measured as a reference to that of the synthesized catalysts. Total organic carbon(TOC) was also measured using Germany multi N/C 3000 analyzer to evaluate the photomineralization degree. The measurements were repeated for each catalytic system, and the experimental error was found to be within the range of ±5%.

The photocatalytic activity of the N-doped TiO_2 can be quantitatively evaluated by comparing the apparent reaction rate constants. The photocatalytic degradation generally follows a Langmuir-Hinshelwood mechanism, with the rate r being proportional to the coverage θ,

$$r = k\theta = kK_C/(1 + K_C) , \quad (1)$$

where k is the true rate constant which includes various parameters such as the mass of catalyst, the intensity of light etc., and K is the adsorption constant. Since the initial concentration is low ($C_0 = 20$ ppm), the term K_C in the denominator can be neglected with respect to unity and the rate becomes, apparently, first order,

$$r = -dc/dt = k K_C = k_a c , \quad (2)$$

where k_a is the apparent rate constant of pseudo-first-order. The integral form $c = f(t)$ of the rate equation is

$$\ln c_0/c = k_a t . \quad (3)$$

2 Results and discussion

2.1 X-ray diffraction with N and F co-doped TiO_2 photocatalyst

Fig. 1 shows the effects of calcination temperature on phase structures of the co-doped TiO_2 powders at 250, 375, 400, 500 and 1000℃. It can be seen that, with increasing calcination temperature (From 250 to 1000℃), the peak intensities of anatase increase and the width of the (101) plane diffraction peak of anatase ($2\theta = 25.4°$) becomes narrower. The co-doped TiO_2 powders only contain anatase phases even at 1000℃. Apparently, ammonium fluoride added retarded phase transformation of the TiO_2 powders from anatase to rutile. The average particle size was estimated by applying the Scherrer formula on the anatase(101) diffraction peaks. An average size of around 8—38 nm was obtained for samples A-E. X-ray structure analysis for samples doped showed the 375℃ samples had typical peaks of TiO_2 polycrystalline anatase nanoparticle without any detectable dopant-related peaks. The dopants went either into the interstitial positions or substitutional sites of TiO_2 crystal structure. The polycrystalline anatase structure was confirmed by (101), (004), (200), (105), and (211) diffraction

peaks. Its tetragonal Bravais lattice type was also verified by lattice constant calculated from these peaks. It is considered, therefore, that the sample annealed at 375℃ is the anatase TiO_2-based polycrystalline powder.

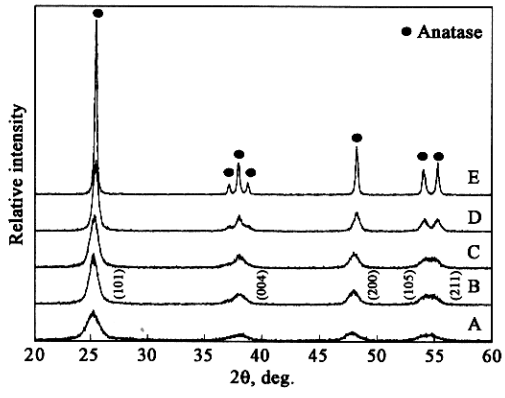

Fig.1 XRD patterns of N and F co-doped TiO_2 powders calcined at (A)250, (B)375, (C)400, (D)500, and (E)1000℃

Fig.2 shows TEM photographs of the co-doped TiO_2 powders prepared by hydrolysis of tetra-butyl titanate in the ammonium fluoride solution calcined at 375℃ for 2 h. The size of the primary particle is about 9 ± 2 nm, which is in agreement with the value determined by XRD(8.8 nm).

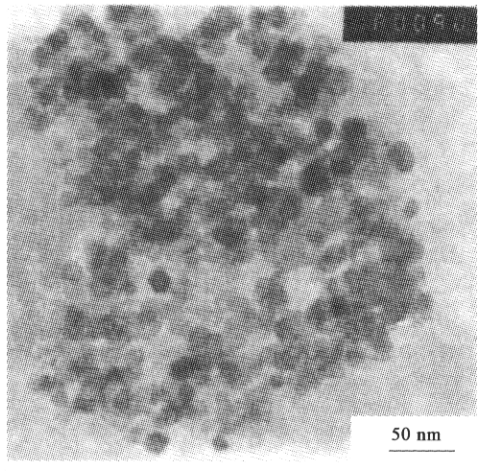

Fig.2 TEM photographs of N and F co-doped TiO_2 powders calcined at 375℃ for 2 h

2.2 BET surface areas and pore structure

Fig.3 shows the pore size distribution curve calculated from the desorption branch of the nitrogen isotherm by the BJH method and the corresponding nitrogen adsorption-desorption isotherms (inset) of co-doped TiO_2 powders calcined at 375℃ for 2 h. The sharp decline in desorption curve is indicative of mesoporosity, while the hysteresis between the two curves demonstrates that there is a diffusion bottleneck, possibly caused by nonuniform pore size. The pore size distribution calculated from the desorption branch of the nitrogen isotherm by the BJH (Barrett-Joyner-Halenda) method shows a narrow range of 4.0—25.0 nm with an average pore diameter of about 15.3 nm. Table 1 shows that all samples prepared by our method have mesoporous structures. Such structures are the result of the pores formed between TiO_2 particles. The diameters of mesopores are several to more than 20 nm. These mesopores allow rapid diffusion of various liquid reactants and products during photocatalytic reaction and enhance the rate of photocatalytic reaction. It can be seen from Table 1, the as-prepared TiO_2 powders dried at 250℃ for 2 h show a very large SBET value of 157.7 m^2/g. However, the surface area and pore volume all become smaller with increasing calcinations temperature. Meanwhile, the pore diameter increases due to the growth of TiO_2 crystallites.

Table 1 Effect of calcination temperature on phase content, BET surface areas and pore parameters of N and F co-doped TiO_2 powders

Sample[a]	Calcinations temp., ℃	Crystallite size[b], nm	Phase	Surface area[c], m^2/m	Pore volume[d], ml/g	Pore size[e], nm
A	250	6.3	A	157.7	0.350	8.9
B	375	8.7	A	89.7	0.343	15.3
C	400	9.4	A	79.5	0.302	19.6
D	500	14.3	A	44.5	0.265	23.0
E	1000	37.5	A			
P25[f]		25.5	A(80%) + R(20%)			

Notes: [a] Doped TiO_2 was prepared by 8 ml of ammonium fluoride(96%) + 20 ml of $Ti(OBu)_4$ by a hydrothermal method; [b] calculated by applying the Scherrer formula on the anatase(101) diffraction peak. A for anatase and R for rutile; [c] BET surface area calculated from the linear part of the BET plot(P/P_0 = 0.05-0.3); [d] total pore volume, taken from the volume of N_2 adsorbed at about P/P_0 = 0.996; [e] average pore diameter, estimated using the adsorption branch of the isotherm and the Barrett-Joyner-Halenda(BJH) formula; [f] see refs(Tahiri, 1996; Fernandez, 2000; Zieli'nska, 2003)

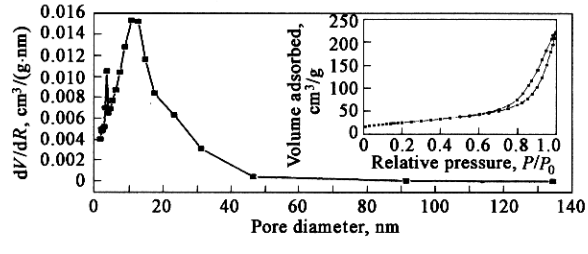

Fig.3 Pore size distribution curve calculated from desorption branch of the nitrogen isotherm by the BJH method and the corresponding nitrogen adsorption-desorption isotherms (inset) of N and F co-doped TiO_2 powders calcined at 375℃ for 2 h

2.3 XPS spectra with N and F co-doped TiO_2 photocatalyst

Fig.4 shows the F 1s and N 1s XPS spectra of the co-doped TiO_2 annealed at 375℃ and raw TiO_2 powders. As shown in Fig. 4(a1), a marked peak at 684.5 eV was observed. Jorda *et al*. (Jorda, 1998) considered that the peaks at 685.3 eV was assigned to formation of TiF_4. Yamaki *et al*. (Yamaki, 2000) concluded the peak at 683.8 eV was assigned to formation of $TiO_{2-x}F_x$ (x = 0.0039). Furthermore, combined with the F 1s binding energy of K_2TiF_6 (685.00 eV) and Na_2TiF_6 (684.90 eV), it was determined that the peak at 684.5 eV was attributed to

formation of Ti-F band and the oxygen atoms were substituted by fluorine atoms. In other words, the XPS spectra illustrated that fluorine atoms had been doped in TiO_2 lattice. In contrast, from Fig.4(b1), the raw TiO_2 powders did not display a peak at 684.5 eV. As shown in Fig.4(a2), the single peak at 400.3 eV was observed. According to Asahi *et al.*(Asahi, 2001), the peak around 400 and 402 eV is the chemisorbed N_2 molecules. In contrast, from Fig.4(b2), the air annealed samples did not display a peak at 396 eV or 397 eV and is raw TiO_2. We concluded that a trace amount of N atoms would be doped at the interstitial sites. Therefore, it is considered that the substitutional fluorine and interstitial nitrogen atoms in co-doped TiO_2 polycrystalline powder were responsible for the vis light response.

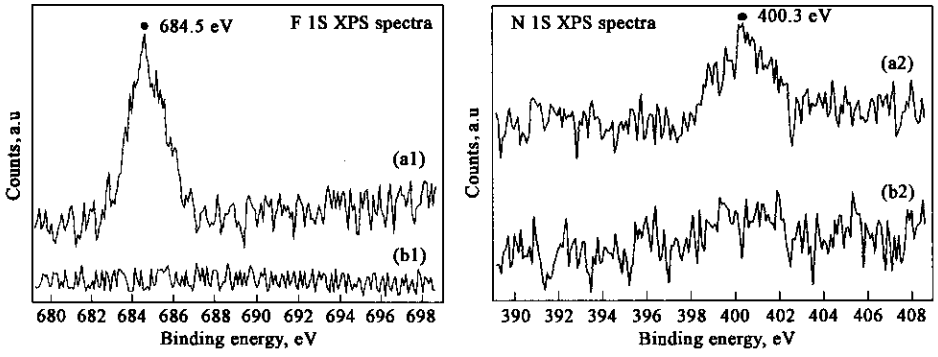

Fig.4 F 1s and N 1s XPS spectra of the (a) N and F co-doped TiO_2 and (b) raw TiO_2

2.4 UV-VIS absorption spectra with N and F co-doped TiO_2 photocatalyst

Optical absorption spectra of the samples are shown in Fig.5. Compared to reference TiO_2 (P25), the absorption edge was shifted to the lower-energy region in the spectrum of the sample annealed at 375℃. Furthermore, the absorption spectra show that the co-doped TiO_2 samples absorb observably from 400 nm to 800 nm wavelengths, whereas reference TiO_2 (P25) samples do not. This clearly indicates a decrease in the band gap energy of the co-doped TiO_2. The narrowing of band gap is due to that N and F doping give rise to a modification of the electronic structure around the conduction band edge of TiO_2.

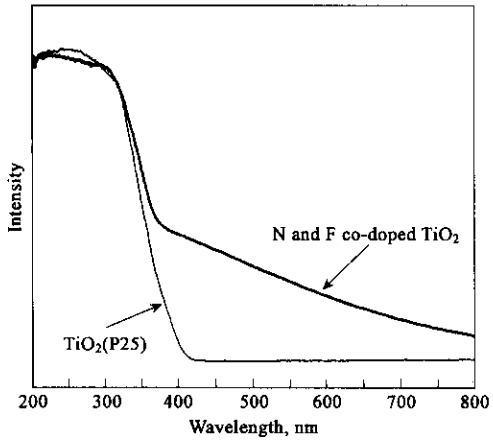

Fig.5 UV-visible diffuse reflectance spectra of N and F co-doped TiO_2 annealed at 375℃ and reference TiO_2 (P25)

2.5 Photocatalytic activity studies

Photocatalytic activity was evaluated by measuring decomposition rates of phenol as a function of irradiation time under 1000 W Xe light ($\lambda > 400$ nm), the 400 nm glass filter was used to assure cutoff of the UV light. Fig.6 shows the dependence of the apparent rate constants (k, min^{-1}) on calcination temperature. The photocatalytic activity of the co-doped TiO_2 calcinated at 375℃ is superior to that of P25 (TiO_2) sample and other doped TiO_2 samples in the visible range of irradiation. The sample calcined at 250℃ shows decent photocatalytic activity with a rate constant of 3.01×10^{-3}. The rate constant increases with increasing calcination temperature. The enhancement of photocatalytic activity at elevated temperatures can be ascribed to an obvious improvement in the crystallinity of anatase (Table 1). At a calcination temperature of 375℃, the k_a reaches the highest value of 3.80×10^{-3}. This rate constant is 2.4 times higher than that of P25 ($k_a = 1.11 \times 10^{-3}$), which is recognized as an excellent photocatalyst (Piscopo, 2001; Tahiri, 1996; Fernandez, 2000). The high photocatalytic activity of the 375℃ sample is partially due to the fact that the co-doped TiO_2 calcinated at 375℃ has smaller particle size and higher adsorption area toward the organic substrate, both of which could be cooperative in making the organic molecular accessible to the active sites on the TiO_2 surface. Moreover, the intense absorption in the visible light range and a red shift in the band gap transition of the co-doped TiO_2 samples are indications that more photogenerated electrons and holes can participate in the photocatalytic reactions. The results of other samples heated at temperatures higher than 500℃ were not shown in this figure because they displayed very poor photocatalytic activity. One possible explanation for this photocatalytic activity decay is that nitrogen and fluorine atoms in TiO_2 lattice were completely substituted by oxygen atoms with calcination temperature rising. Therefore, we concluded that 375℃ was the transition temperature, at

which the co-doped TiO_2 photocatalyst could have suitable band gap by N and F co-doping and the recombinations of the light-induced electron(s) (e^-) and hole(s) (h^+) could be restrained furthest and resulted in the highest vis-activity. Since P-25 is considered as an excellent photocatalyst, 240% enhancement is certainly significant for phenol decomposition under visible light(wavelength < 700 nm).

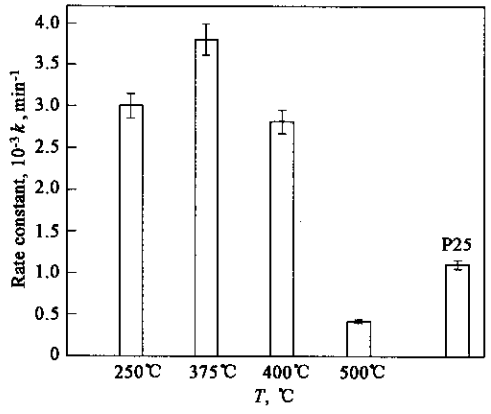

Fig. 6 The dependence of the apparent rate constants (k, min^{-1}) on calcination temperature

3 Conclusions

A simple method was developed for the preparation of highly photoactive nanocrystalline N and F co-doped TiO_2 photocatalysts by calcination of the hydrolysis product of tetrabutyl titanate with ammonium fluoride.

The co-doped TiO_2 powders only contain anatase phases even at 1000℃. Apparently, ammonium fluoride added retarded phase transformation of the TiO_2 powders from anatase to rutile.

The substitutional fluorine and interstitial nitrogen atoms in co-doped TiO_2 polycrystalline powder were responsible for the vis light response.

The N and F co-doped TiO_2 samples showed stronger absorption in the visible range and a red shift in the band gap transition.

The photocatalytic activity of N and F co-doped TiO_2 powders with anatase phases calcined at 375℃ is 2.4 times higher than that of Degussa P25 for phenol decomposition under visible light.

Acknowledgements: The authors thank Mr. Weijing Yin and Ms. Ruibin Wang of the Instrumental Analysis Center, Shanghai Jiaotong University for their assistance in measurements of the XRD spectra.

References:

Asahi R, Morikawa T, Ohwaki K *et al*., 2001. Visible-light photocatalysis in nitrogen-doped titanium oxides[J]. Science, 293: 269-271.

Choi W, Termin A, Hoffmann M R, 1994. Role of metal ion dopants in quantum-sized TiO_2 correlation between photoreactivity and charge carrier recombination dynamics[J]. J Phys Chem, 98: 13669—13679.

Fernandez A, Lassaletta G, Jimenez V M *et al*., 1995. Preparation and characterization of TiO_2 photocatalysts supported on various rigid supports (glass, quartz and stainless steel). Comparative studies of photocatalytic activity in water purification[J]. Applied Catalysis B: Environmental, 7: 49—59.

Fernandez-Ibanez P, de las Nieves F J, Malato S, 2000. Titanium dioxide/electrolyte solution interface: Electron transfer phenomena[J]. J Colloid Interface Sci, 227(2): 510—516.

Fujishima A, Honda K, 1972. Electurochemical photolysis of water at a semiconductor electrode[J]. Nature, 238: 37—38.

Herrmann J M, Disdier J, Courbon H, 1984. Modification of the TiO_2 electron density by ion doping or metal deposit and consequences for photoassisted reactions[J]. Chem Phys Lett, 108: 319—326.

Iwasaki M, Hara M, Kawada H *et al*., 2000. Cobalt ion-doped TiO_2 photocatalyst response to visible light[J]. Journal of Colloid and Interface Science, 224(1): 202—204.

Jorda E, Tuel A, Teissiery R *et al*., 1998. Synthesis, characterization, and activity in the epoxidation of cyclohexene with aqueous H_2O_2 of catalysts prepared by reaction of TiF_4 with silica[J]. J Catal, 175: 93—107.

Karakitsou K E, Verykios X E, 1993. Effects of altervalent cation doping of TiO_2 on its performance as a photocatalyst for water cleavage[J]. J Phys Chem, 97: 1184—1189.

Khan S U M, Mofareh Al-Shahry, William B *et al*., 2002. Efficient photochemical water splitting by a chemically modified n-TiO_2[J]. Science, 297: 2243—2245.

Piscopo A, Robert D, Weber J V, 2001. Comparison between the reactivity of commercial and synthetic TiO_2 photocatalysts[J]. J Photochem Photobiol A: Chem, 139: 253—256.

Tahiri H, Serpone N, LevanMao R, 1996. Application of concept of relative photonic efficiencies and surface characterization of a new titania photocatalyst designed for environmental remediation[J]. J Photochem Photobiol A, 93: 199—203.

Umebayashi T, Yamaki T, Itoh H *et al*., 2002. Band gap narrowing of titanium dioxide by sulfur doping[J]. Applied Physics Letters, 81: 454—457.

Yamashita H, Ichihashi Y, Takeuchi M *et al*., 1999. Characterization of metal ion-implanted titanium oxide photocatalysts operating under visible light irradiation[J]. J Synchrotron Radia, 6: 451—452.

Yamashita H, Ohshiro S, Anpo M *et al*., 2001. Visible-light-responsive photocatalytic reaction on tetrahedrally-coordinated chromium oxide moieties loaded on ZSM-5 zeolites and HMS mesoporous silica: Partial oxidation of propane[J]. Research on Chemical Intermediates, 29: 881—890.

Yamaki T, Sumita T, Yamamoto S, 2002. Formation of $TiO_{2-x}F_x$ compounds in fluorine-implanted TiO_2[J]. J Mater Sci Lett, 21: 33—35.

Yamaki T, Umebayashi T, Sumita T *et al*., 2003. Fluorine-doping in titanium dioxide by ion implantation technique[J]. Nucl Instr and Meth in Phys Res (B), 206: 254—258.

Zieli'nska B, Grzechulska J, Morawski A, 2003. Photocatalytic decomposition of textile dyes on TiO_2-Tytanpol A11 and TiO_2-Degussa P25[J]. J Photochem Photobiol A: Chem, 157: 65—70.

(Received for review March 4, 2004. Accepted June 7, 2004)